29. D. Troilo, M. D. Gottlieb, J. Wallman, *Soc. Neurosci. Abstr.* **12**, 120 (1986); C. Wildsoet and J. D. Pettigrew, personal communication.
30. D. Troilo, M. D. Gottlieb, J. Wallman, *Invest. Ophthalmol. (ARVO Suppl.)* **28**, 263 (1987).
31. B. M. Glaser, P. A. D'Amore, R. G. Michels, A. Patz, A. Fenselau, *J. Cell Biol.* **84**, 298 (1980); G. A. Lutty *et al.*, *J. Cell Sci.* **76**, 53 (1985).
32. C. E. Ferree, G. Rand, C. Hardy, *Am. J. Ophthalmol.* **15**, 513 (1932); G. L. Walls, *The Vertebrate Eye and its Adaptive Radiations* (Cranbrook Institute of Science, Bloomfield Hills, NJ, 1942); J. G. Sivak, *Vision Res.* **16**, 945 (1976).
33. M. Millodot, *Am. J. Optom. Physiol. Opt.* **58**, 691 (1981).
34. F. W. Fitzke, B. P. Hayes, W. Hodos, A. L. Holden, J. C. Low, *J. Physiol. (London)* **369**, 33 (1985).
35. The relevant factor is the size of saccades relative to the size of the stimuli after filtering by the spatial characteristics of the neuron. Since most saccades during either free-viewing or reading are larger than most retinal receptive fields [A. T. Bahill, D. Adler, L. Stark, *Invest. Ophthalmol. Visual Sci.* **14**, 468 (1975); D. Heller and A. Heinisch, in *Eye Movements and Human Information Processing*, R. Groner, G. W. McConkie, C. Menz, Eds. (Elsevier, New York, 1985)], the distribution of spatial frequencies in the visual scene is the more important variable.
36. Each point on this figure is an estimate of the output of a retinal ganglion cell with the center of its receptive field at that point. Each receptive field is treated as an excitatory central process and an inhibitory surround process, both Gaussian in shape, with the receptive field diameter declining linearly with distance from the fovea. To obtain each point, Dr. C. M. Harris and I multiplied the brightness of the scene at each location in each receptive field by the height at that point of the curve representing the difference between the influence of the excitatory center and the inhibitory surround and summed all of these points. The result of these computations constitutes what might be called the "ganglion cells' view" of the scene. For printed text, the image is distinct only around the fovea and becomes blurred quite quickly with distance from the fovea. For the change in receptive field size with eccentricity, we used the figures of Blakemore and Vital-Durand [C. Blakemore and F. Vital-Durand, *Trans. Ophthalmol. Soc. U.K.* **99**, 363 (1979)] for the lateral geniculate neurons of the rhesus monkey, but multiplied by 1.33 to reflect the larger size of human eyes. For the size of the foveal receptive fields, we used 0.02°. For the shape of the center and surround processes, we considered the surround to have an area ten times that of the center and a total influence half as great as the center (Robert Shapley, personal communication). The page analyzed here was regarded as subtending 50°.
37. F. M. de Monasterio, *J. Neurophysiol.* **41**, 1394 (1978); R. Shapley, V. H. Perry, *Trends Neurosci.* **9**, 229 (1986).
38. S. G. Crewther, J. Nathan, P. M. Kiely, N. Brennan, D. P. Crewther, *Invest. Ophthalmol. (ARVO Suppl.)* **27**, 202 (1986). A similar experiment by Smith and colleagues in which the kittens wore the lenses for 2 hours each day and spent the remaining time in the dark did produce myopia (*6*).
39. J. Nathan, S. G. Crewther, D. P. Crewther, P. M. Kiely, *Invest. Ophthalmol. Visual Sci.* **25**, 1300 (1984).
40. R. Shapley and C. Enroth-Cugell, *Prog. Retinal Res.* **3**, 263 (1984).
41. We thank R. Shapley, C. M. Harris, J. C. Letelier, and M. Stryker for valuable discussions about the properties of retinal ganglion cells and D. Troilo, J. C. Letelier, F. A. Miles, and L. Wise for critical comments on this manuscript. Supported by NIH grant EY02727. V.R. was supported by the College Research Scholars program of City College.

4 August 1986; accepted 27 March 1987

Localization of Amyloid β Protein Messenger RNA in Brains from Patients with Alzheimer's Disease

SINA BAHMANYAR, GERALD A. HIGGINS, DMITRY GOLDGABER, DAVID A. LEWIS, JOHN H. MORRISON, MICHAEL C. WILSON, SUSARLA K. SHANKAR, D. CARLETON GAJDUSEK

The distribution of cells containing messenger RNA that encodes amyloid β protein was determined in hippocampi and in various cortical regions from cynomolgus monkeys, normal humans, and patients with Alzheimer's disease by in situ hybridization. Both ^{35}S-labeled RNA antisense and sense probes to amyloid β protein messenger RNA were used to ensure specific hybridization. Messenger RNA for amyloid β protein was expressed in a subset of neurons in the prefrontal cortex from monkeys, normal humans, and patients with Alzheimer's disease. This messenger RNA was also present in the neurons of all the hippocampal fields from monkeys, normal humans and, although to a lesser extent in cornu ammonis 1, patients with Alzheimer's disease. The distribution of amyloid β protein messenger RNA was similar to that of the neurofibrillary tangles of Alzheimer's disease in some regions, but the messenger RNA was also expressed in other neurons that are not usually involved in the pathology of Alzheimer's disease.

WE HAVE USED THE COMPLEMENTARY DNA (cDNA) clone λAm4 (*1*) encoding amyloid β protein (*1–4*) as a template to generate ^{35}S-labeled RNA probes for localization by in situ hybridization of the messenger RNA (mRNA) encoding amyloid β protein in the cerebral cortex and hippocampus of cynomolgus monkeys, normal human subjects, and patients with Alzheimer's disease (AD). We found that, in all cases, the mRNA encoding amyloid β protein was expressed in specific subpopulations of neurons in the neocortex and hippocampus. In some regions, the size and laminar distribution of these neurons were similar to those of the subset of neurons that develop neurofibrillary tangles (NFT) in AD. But the mRNA encoding amyloid β protein was also expressed in the neurons of other regions of the neocortex and hippocampus that are relatively preserved in AD.

The cortical distribution patterns of NFT and neuritic plaques (NP) suggest that certain cortical cell types and their associated circuits are devastated in AD, whereas others are spared (*5–9*). In addition, certain cytoskeletal proteins, as well as the amyloid β protein, have been implicated in NFT and NP formation (*10*). It has been suggested that the fibrillary amyloid deposits that are present in intracellular NFT, extracellular NP, and the cerebral vasculature in AD all arise from the same amyloid β protein (*2, 11, 12*). In addition, this same protein occurs in the NFT and NP in brains of patients with Down syndrome (*11, 13*). The vascular and extracellular amyloid might enter the brain from the circulation (*14*); however, the recent molecular characterization of am-

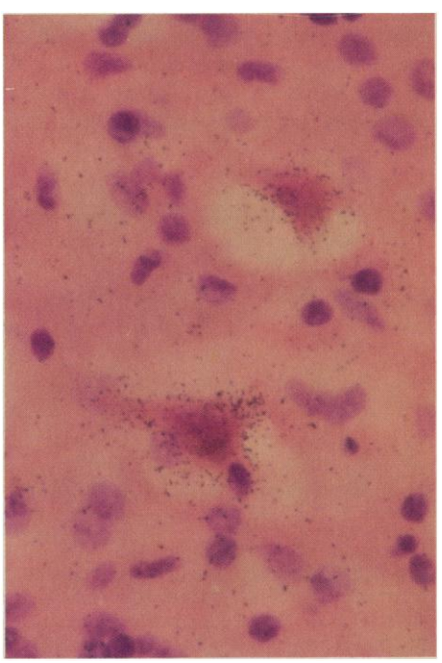

Fig. 1. In situ hybridization of amyloid β protein mRNA in the superior frontal gyrus from a patient with Alzheimer's disease (counterstained with cresyl violet and eosin). Note preferential cellular labeling (dark silver grains) on pyramidal cells of layer V.

S. Bahmanyar, D. Goldgaber, S. K. Shankar, D. C. Gajdusek, Laboratory of Central Nervous System Studies, National Institute of Neurological and Communicative Disorders and Stroke, National Institutes of Health, Bethesda, MD 20892.
G. A. Higgins and M. C. Wilson, Department of Molecular Biology, Scripps Clinic and Research Foundation, La Jolla, CA 92037.
D. A. Lewis and J. H. Morrison, Department of Basic and Clinical Research, Scripps Clinic and Research Foundation, La Jolla, CA 92037.

yloid β protein and preliminary analysis of its distribution suggest that the mRNA coding for a putative precursor to the amyloid β protein is present in both the central nervous system and several peripheral organs (*1, 3*).

Brain tissue for in situ hybridization was obtained from three cynomolgus monkeys (*Macaca fascicularis*), from three adults with no neurological disorders, and from two patients in whom neuropathological evaluation confirmed the clinical diagnosis of AD (*15, 16*). Transcription of ^{35}S-labeled RNA probes (*17*) and in situ hybridization (*18*) was performed as described. To provide a probe for detection of amyloid β protein mRNA, a 1-kb Eco RI restriction fragment from the human brain cDNA clone λAm4 encoding amyloid β protein was subcloned in the pGEM-3 plasmid (Promega Biotech) (*1*). T7 RNA polymerase was used for generation of the antisense probe, and SP6 RNA polymerase was used for generation of sense probe. In addition, SP6 RNA transcripts homologous to mouse proteolipid protein mRNA were generated from the pMuBr2 plasmid vector (*19*) to serve as an oligodendrocyte-specific marker.

Tissue sections from neocortex and hippocampus from monkeys, normal humans, and patients with AD incubated with the antisense strand complementary to amyloid β protein mRNA showed extensive cellular labeling, as evidenced by clustered silver grains (Fig. 1). To ensure that the signal obtained with antisense probe reflected the presence of amyloid β protein mRNA and was not due to nonspecific effects of RNA or cellular density (*20*), control hybridizations were performed with both a sense probe of amyloid β protein mRNA (Fig. 2, A through D) and an antisense probe complementary to proteolipid protein mRNA (*19*). Sense strand hybridizations, with a probe of the same mass and specific activity as that used in the antisense hybridization, failed to produce any discernible cellular hybridization in any of the tissues (Fig. 2). Antisense probe hybridization with the proteolipid probe produced positive hybridization within oligodendrocytes, especially in white matter, but no hybridization was apparent within neurons.

In area 9 (dorsomedial convexity) and area 46 (principal sulcus) of the cynomolgus prefrontal cortex, labeled cells were present in all six layers, with a distinctive laminar pattern of cell density and size. In both areas, superficial layer V (VA) consistently had the greatest density of labeled cells. The deep portion of layer III also had a high density of labeled cells, although it was consistently lower in density than superficial layer V (Fig. 3A). The overall cellular density of layer IV (as seen in a conventional Nissl stain) is much higher than that of layers III or V; however, when the hybridized sections were counterstained with cresyl violet, it was evident that layers V and III contain the highest density of grain clusters due to selective hybridization of these neurons and not to a higher cell density. Layer II, superficial layer III, and deep layer V had the next highest density, followed by layers IV and VI. Layer I only occasionally contained cellular labeling.

The superior frontal gyrus of normal human brain also contained numerous labeled cells in layers II through VI; the highest density of labeled cells was in the infragranular layers (V and VI), although laminar differences in the density of labeled cells were less distinct than in monkey prefrontal cortex (Fig. 3B).

The superior frontal gyrus of brains from patients with AD also contained dense grain clusters suggestive of cellular labeling, and the laminar pattern was similar to that of cynomolgus monkey and normal human brain in that layer V had the highest density of grain clusters (Fig. 3C). However, the relative density of labeling in layer III was lower than in the same region of normal human cortex. The lower density of labeled cells in layer III may reflect the neuronal loss in AD brain. On one section from superior frontal gyrus of brain from a patient with AD, the cellular grain clusters had the following laminar densities: layer I, 19 clusters/mm^2; layers II through IV, 137 clusters/mm^2; layer V, 309 clusters/mm^2; and layer VI, 104 clusters/mm^2. In the same region of normal human brain, laminar densities for layer V showed no significant difference, but the densities of layers II through IV were constantly 30 to 50% higher than in AD brain. Adjacent sections stained for thioflavine-S showed that superficial layer V also had the highest density of NFT in this case of AD.

Within the hippocampal formation of cynomolgus monkey, neurons in the pyramidal cell layer of all cornu ammonis (CA) fields exhibited a strong hybridization signal. In CA3, occasional cells in the stratum oriens were also labeled. The CA fields contained dense grain clusters, indicative of cellular hybridization that reflect the distribution of large pyramidal neurons (Fig. 4, A and B). Examination of normal human hippocampal formation showed similar abundant expression of amyloid β protein mRNA within all the CA fields (Fig. 4, C and D). Unlike normal human and monkey hippocampus, where the hybridization signal was high in both CA3 and CA1, in AD hippocampus there were fewer grain clusters in CA1 than in CA3 (Fig. 4, E and F). The difference in CA1 neuronal density and consequent loss of amyloid β protein mRNA hybridization was due to the selective loss of neurons within CA1 in AD (*21*). This interpretation was supported by the Nissl-stained sections of AD hippocampus (Fig. 4F). The results of in situ hybridization were constant and reproducible in all of the normal control or AD brain tissue.

These data have several implications for the cellular pathology of AD. First, the mRNA encoding amyloid β protein is present in neurons of normal cynomolgus monkey brain, normal human brain, and brains from patients with AD. This finding suggests that the mRNA for the precursor protein that is the source of pathologic

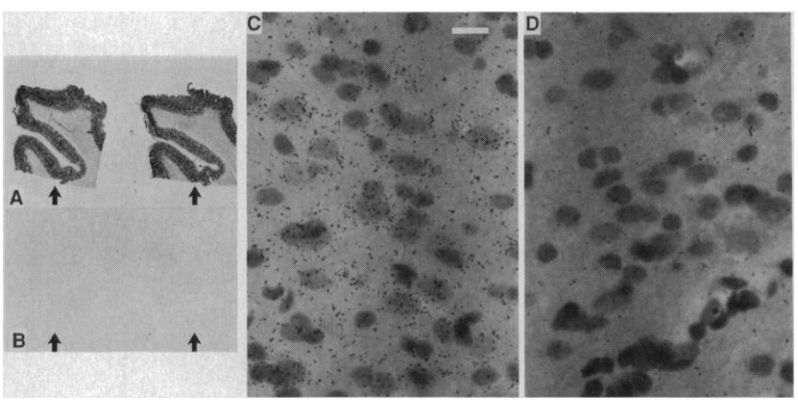

Fig. 2. Specificity of in situ hybridization with the amyloid β protein probe. (**A** and **B**) Adjacent coronal tissue sections of frontal cortex from normal human brain were hybridized with either ^{35}S-labeled (A) antisense RNA probe complementary to amyloid β protein mRNA or (B) sense strand RNA probe for the amyloid mRNA. Photographs of x-ray film images at ×4 magnification with the position of tissue sections indicated by arrows show (A) specific hybridization with antisense RNA probe and (B) lack of specific hybridization with sense strand RNA probe. (**C** and **D**) Adjacent coronal tissue sections of frontal cortex from cynomolgus monkey brain were hybridized with either ^{35}S-labeled (C) antisense RNA probe complementary to amyloid β protein mRNA or (D) sense strand RNA probe for the amyloid mRNA. Hybridized slides were counterstained with cresyl violet and eosin, photomicrographs at ×200 show (C) specific hybridization with antisense RNA probe and (D) lack of specific hybridization with sense strand RNA probe. Calibration bar, 32 μm.

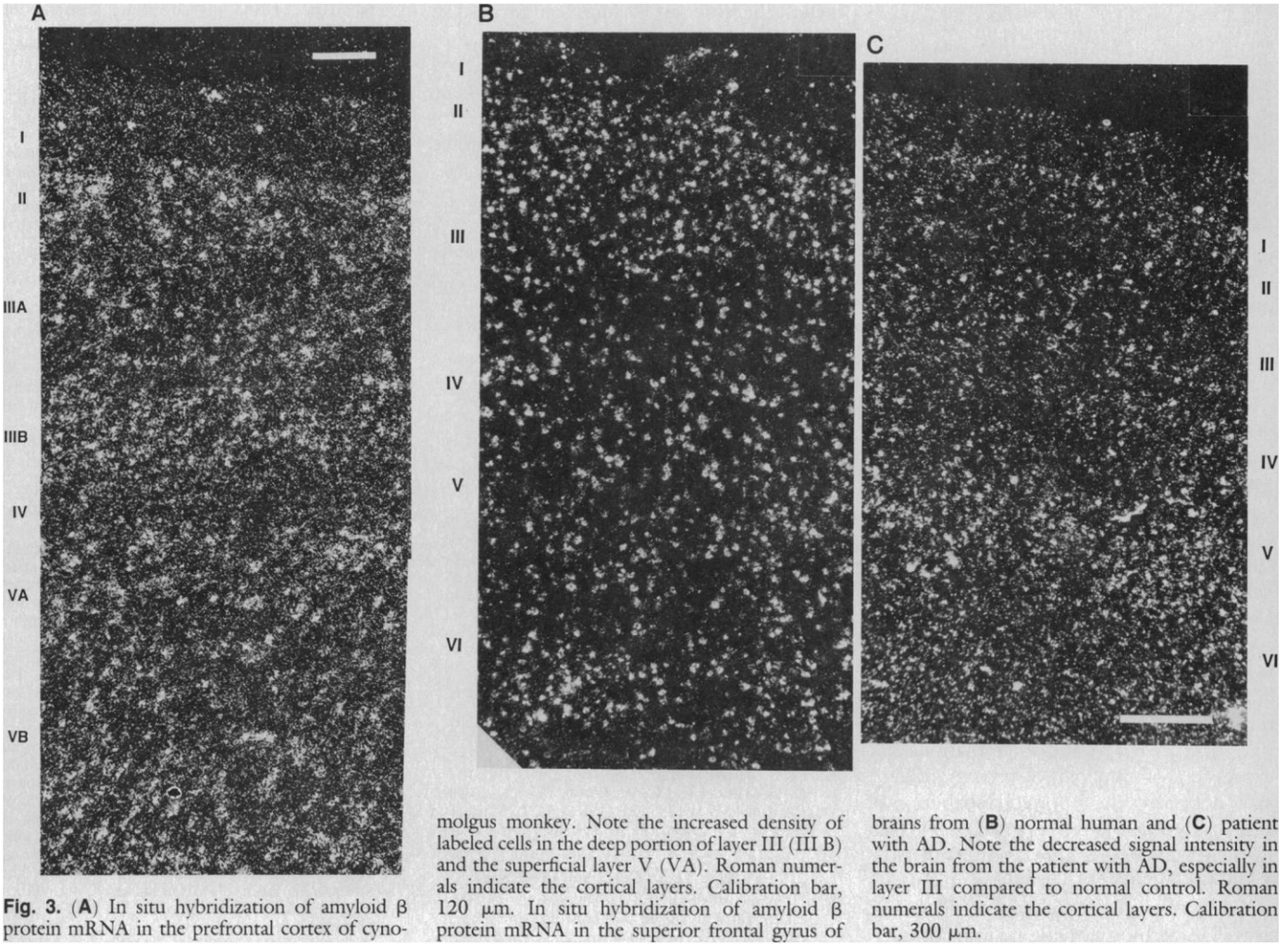

Fig. 3. (**A**) In situ hybridization of amyloid β protein mRNA in the prefrontal cortex of cynomolgus monkey. Note the increased density of labeled cells in the deep portion of layer III (III B) and the superficial layer V (VA). Roman numerals indicate the cortical layers. Calibration bar, 120 μm. In situ hybridization of amyloid β protein mRNA in the superior frontal gyrus of brains from (**B**) normal human and (**C**) patient with AD. Note the decreased signal intensity in the brain from the patient with AD, especially in layer III compared to normal control. Roman numerals indicate the cortical layers. Calibration bar, 300 μm.

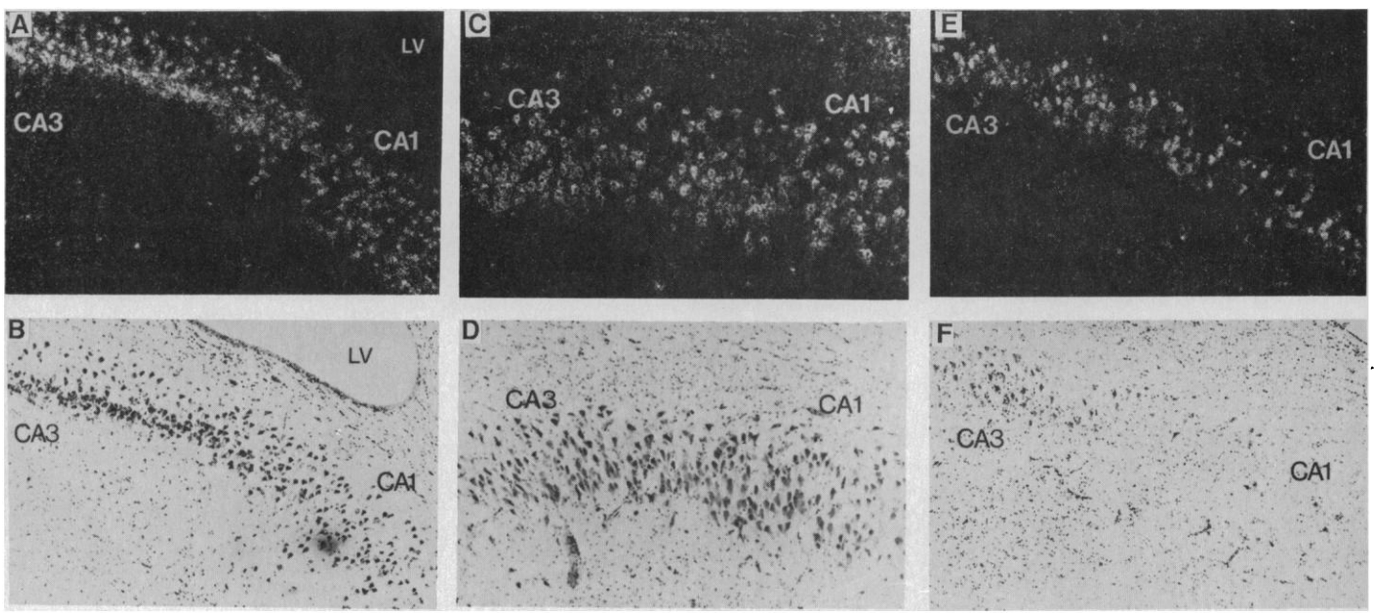

Fig. 4. In situ hybridization of amyloid β protein mRNA in pyramidal neurons of the hippocampal formation. Dark-field photomicrographs of the hippocampal formation show that amyloid β protein mRNA is expressed approximately equally in cells of the CA3 field, the transition zone of CA2, and in CA1 of a cynomolgus monkey (LV, lateral ventricle) (**A** and **B**), an age-matched normal human (**C** and **D**), and a patient with AD (**E** and **F**). Nissl-stained sections confirm that apparently all of the large pyramidal neurons in the CA fields in monkey (B), normal human (D), and the patient with AD (F) contain the mRNA. Note the relatively decreased signal intensity in the CA1 field from the AD patient (E) due to neuronal loss, as shown in the Nissl-stained section (F).

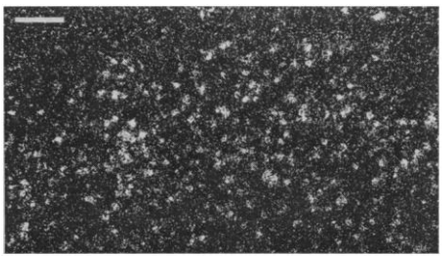

Fig. 5. In situ hybridization of amyloid β protein mRNA in the infragranular layers (V and VI) of primary visual cortex (Brodmann's area 17) of normal human brain. Note the presence of labeled cells in this region of brain, which lacks neurofibrillary tangles in Alzheimer's disease. Calibration bar, 120 μm.

amyloid protein in AD is a natural constituent of certain cortical cells. Further, the mRNA for this protein does not appear to be present in all cells and, at least in prefrontal cortex, it is preferentially expressed by the large pyramidal cells of layers III and V. The large pyramidal neurons of these layers are also prone to NFT formation and degeneration in AD (*5, 22*). However, this correlation between the pathology of AD and amyloid β protein mRNA distribution is not evident in all brain regions. For example, in the hippocampal formation, the expression of amyloid β protein mRNA does not reflect the reported distribution of neuropathological markers in AD (*21*). That is, in AD, there are large amounts of amyloid β protein mRNA within pyramidal cells of CA3, a region relatively preserved in AD, as well as within surviving neurons of CA1. A similar distribution is apparent within the CA fields of cynomolgus monkey and within the dentate gyrus and temporal cortices of both species (*23*). In addition, although the primary visual cortex in AD brains contains almost no NFT (*5, 8*), it does contain positively hybridizing neurons in layers V and VI (*24*) (Fig. 5). Thus, it appears that certain neurons can express a high level of amyloid β protein and yet be spared the overt pathology of cell loss and amyloid complex deposition in AD. Purkinje cells of the cerebellum, and a class of glial cells, oligodendrocytes, also express the amyloid β protein mRNA (*25*).

The presence or absence of an additional molecular factor in the affected cells may confer vulnerability. For example, in both normal human and monkey prefrontal cortex, neurons with anatomical characteristics similar to those containing amyloid β protein mRNA also contain high levels of nonphosphorylated neurofilament protein, which has also been implicated in the cellular pathology of AD (*6*). The pyramidal neurons, which appear to be vulnerable to NFT formation in AD, may require the combined expression of several related genes. Because duplication of amyloid β protein gene (*26*) on chromosome 21 (*1–3, 27*) may be the genetic defect in Alzheimer's disease, the aberrant regulation of this gene product could selectively damage certain neurons, depending on the molecular profile of the neuronal cell type.

REFERENCES AND NOTES

1. D. Goldgaber *et al.*, in *Alzheimer's Disease: Advances in Basic Research Therapies* (Center of Brain Sciences and Metabolism Charitable Trust, Cambridge, MA, 1987), pp. 209–217; D. Goldgaber, M. I. Lerman, O. W. McBride, U. Saffioti, D. C. Gajdusek, *Science* **235**, 877 (1987).
2. J. Kang *et al.*, *Nature (London)* **325**, 733 (1987).
3. R. E. Tanzi *et al.*, *Science* **235**, 880 (1987).
4. N. K. Robakis *et al.*, *Proc. Natl. Acad. Sci. U.S.A.*, in press.
5. D. A. Lewis *et al.*, *J. Neurosci.*, in press.
6. J. H. Morrison *et al.*, *Brain Res.*, in press.
7. D. M. A. Mann and P. O. Yates, *Hum. Neurobiol.* **5**, 147 (1986).
8. R. C. A. Pearson, M. M. Esiri, R. W. Hiorns, G. K. Wilcock, T. P. S. Powell, *Proc. Natl. Acad. Sci. U.S.A.* **82**, 4531 (1985).
9. C. Q. Mountjoy, *Br. Med. Bull.* **42**, 81 (1986).
10. D. C. Gajdusek, *N. Engl. J. Med.* **312**, 714 (1985); I. Grundke-Iqbal *et al.*, *Proc. Natl. Acad. Sci. U.S.A.* **83**, 4913 (1986); K. Iqbal *et al.*, *Lancet* **1986-II**, 421 (1986); K. S. Kosik *et al.*, *Proc. Natl. Acad. Sci. U.S.A.* **81**, 7941 (1984); G. Perry, N. Rizzuto, L. Autilio-Gambetti, P. Gambetti, *ibid.* **82**, 3916 (1985) D. J. Selkoe, D. S. Bell, M. B. Podlisny, D. L. Price, L. C. Cork, *Science* **235**, 873 (1987); D. Guiroy *et al.*, *Proc. Natl. Acad. Sci. U.S.A.* **84**, 2073 (1987).
11. K. Beyreuther *et al.*, *Disc. Neurosci.* **3**, 68 (1986).
12. C. L. Masters *et al.*, *EMBO J.* **4**, 2757 (1985).
13. G. G. Glenner and C. W. Wong, *Biochem. Biophys. Res. Commun.* **122**, 1131 (1984); C. L. Masters *et al.*, *Proc. Natl. Acad. Sci. U.S.A.* **82**, 4245 (1985); C. W. Wong, V. Quaranta, G. G. Glenner, *ibid.*, p. 8729.
14. G. G. Glenner, *Hum. Pathol.* **16**, 433 (1985).
15. Human brains from three adults with no neurological disorders and from two patients with a clinical diagnosis of AD were analyzed. The clinical diagnosis in both cases of AD was confirmed by neuropathological evaluations that revealed atrophy and the presence of both NFT and NP in multiple regions of the neocortex and hippocampus. Brain tissues were removed within 1.5 hours of death, placed in 4% paraformaldehyde for 48 hours, and then processed (*16*). For both monkey and human brains, alternate sections and some hybridized sections were stained with cresyl violet. Cytoarchitectonic regions were identified according to published criteria [K. Brodmann, *Lokalisationslehre der Grosshirnrinde* (J. A. Barth, Leipsiz, 1909); A. E. Walker, *J. Comp. Neurol.* **73**, 59 (1940)]. The following areas were examined: the superior frontal gyrus (Brodmann area 9) from human brain and Walker's areas 9 and 46 from cynomolgus monkey, as well as corresponding regions of the hippocampal formation.
16. Three young adult male cynomolgus monkeys (*Macaca fascicularis*) were used for in situ hybridization. Animals were perfused and brain tissue prepared as described [D. A. Lewis, M. J. Campbell, S. L. Foote, M. Goldstein, J. H. Morrison, *J. Neurosci.* **7**, 279 (1987)]. Briefly, animals were deeply anesthetized with ketamine hydrochloride (25 mg per kilogram of body weight, intramuscularly) and pentobarbital sodium (10 mg per kilogram of body weight, intraperitoneally). An endotracheal tube was inserted and mechanical ventilation with 100% oxygen was initiated. After the chest was opened, 1.5 to 2.0 ml of 1% aqueous sodium nitrite was injected into the left ventricle of the heart. Animals were then perfused transcardially with cold 1% paraformaldehyde in 0.15*M* phosphate-buffered saline (PBS) for 30 to 60 seconds followed by perfusion with cold 4% paraformaldehyde in PBS. The latter solution was perfused for 8 to 10 minutes at a flow rate of 250 to 500 ml/min, depending upon the size of the animal. Immediately after the perfusion, the brain was removed and sliced into blocks, 3 to 5 mm thick, which were placed in cold fixative for an additional 6 hours. Tissue blocks were then washed in a series of cold, graded sucrose solutions, and sectioned coronally in a cryostat at 20 μm. Tissue sections were then mounted on gelatin-coated slides, air-dried, and stored at either 4°C for 1 to 3 days or at −70°C for up to 4 weeks before use.
17. Transcription was performed in 40 m*M* tris-HCl, *p*H 7.5, 6 m*M* $MgCl_2$, 2 m*M* dithiothreitol, 5 units of ribonuclease inhibitor (Promega Biotech), 400 μ*M* adenosine triphosphate and cytidine triphosphate, 25 μ*M* [^{35}S]guanosine 5′-(α-thio)triphosphate and [^{35}S]uridine 5′-(α-thio)triphosphate (800 to 1000 Ci/mmol, NEN), 1 to 2 μg of linearized DNA template, plus 5 to 10 units of SP6 RNA polymerase (Boehringer Mannheim) or T7 RNA polymerase (Stratagene Cloning Systems). Transcription was carried out at 37°C for 1 to 2 hours. Incorporation was measured by trichloroacetic acid precipitation, with typical values of 20 to 50% incorporation, yielding 50 to 100 ng of probe with a specific activity greater than 2×10^9 cpm/μg. No attempt was made to remove DNA template by deoxyribonuclease treatment, as we have observed that the presence of nondenatured template does not diminish in situ hybridization.
18. In situ hybridization was performed as described (*20*). Slide-mounted sections were "postfixed" in 4% paraformaldehyde in PBS for 5 minutes at room temperature and then rinsed twice in PBS. Slides were immersed in proteinase K (50 μg/ml) (Boehringer Mannheim) in 5× TE (10 m*M* tris, 1 m*M* EDTA, *p*H 8) for 7.5 minutes at room temperature, rinsed in PBS, placed in 0.05*N* HCl for 7.5 minutes, then rinsed and dehydrated in graded alcohols containing 0.33*M* ammonium acetate, and air-dried at room temperature. Approximately 750 μl of buffer A, containing 0.75*M* NaCl, 0.1*M* 1,4-piperazinediethanesulfonic acid (Pipes) buffer, 0.1*M* EDTA, 5× Denhardt's (1% bovine serum albumin, 1% Ficoll, and 1% polyvinylpyrrolidone), 50 m*M* dithiothreitol, 0.2% SDS, 10% dextran sulfate, denatured yeast RNA (500 μg/ml), and salmon sperm DNA (500 μg/ml) was applied to the tissue sections on slides laying flat, which were placed in a humidified, sealed chamber at 48°C for 2 to 3 hours. Subsequently, this buffer was removed, and 75 μl of hybridization buffer containing 5 ng of probe in buffer A was applied to the slides. Cover slips were placed on the slides and sealed with waterproof contact cement (Royalbond Grip Cement). The slides were again placed in a sealed, humidified chamber for overnight hybridization at 48°C. After hybridization, coverslips were removed in 4× standard saline citrate (SSC, 0.15*M* NaCl and 0.15*M* sodium citrate) containing 300 m*M* β-mercaptoethanol. After a rinse step in 4× SSC without β-mercaptoethanol, the sections were digested with pancreatic ribonuclease (50 μg/ml) in 0.5*M* NaCl and 1× TE buffer for 30 minutes at 37°C. This was followed by a 30-minute incubation in the same buffer without ribonuclease at 37°C, and a series of low-salt rinses at elevated temperature (2× SSC at 56°C, followed by 0.5× SSC at 42°C). The slides were air-dried and exposed to x-ray film (DuPont Cornex 5) for 48 to 72 hours at room temperature. The slides were then dipped in emulsion (Kodak NTB-2), exposed for 5 to 10 days, and developed for autoradiography.
19. P. Branks and M. C. Wilson, *Mol. Brain Res.* **1**, 1 (1986).
20. G. A. Higgins and M. C. Wilson, in *In Situ Hybridization: Applications to Neurobiology*, K. Valentino, J. Eberwine, J. Barchas, Eds. (Oxford University Press, New York, 1987).
21. B. T. Hyman *et. al.*, *Science* **225**, 1168 (1984); B. T. Hyman *et al.*, *Ann. Neurol.* **20**, 472 (1986).
22. R. D. Terry, A. Pelk, R. De Teresa, R. Schecter, D. S. Horoupian, *Ann. Neurol.* **10**, 184 (1981); D. M. A. Mann, P. O. Yates, B. Marcyniuk, *Neurosci. Lett.* **56**, 51 (1985).
23. G. A. Higgins *et al.*, in preparation.
24. D. A. Lewis *et al.*, in preparation.
25. D. E. Schmechel *et al.*, in preparation.
26. J. M. Delabar *et al.*, *Science* **235**, 1390 (1987).
27. N. K. Robakis *et al.*, *Lancet* **1987-I**, 384 (1987); P. H. St George-Hyslop *et al.*, *Science* **235**, 885 (1987).

28. Supported by the Hereditary Disease Foundation, the Alzheimer's Disease and Related Disorders Association, and grants NIA AG05131, NIMH RSDA MH00519, and NIH NS23038. We thank M. L. Dietrich and N. S. Callahan for expert secretarial assistance.

10 March 1987; 14 May 1987